TASK I

Project I.6

FERRIC SULFIDE AS A PRECURSOR FOR COAL LIQUEFACTION CATALYSTS AND SURFACE STUDIES OF ACTIVITY AND SELECTIVITY

A.H. Stiller, J.-P. Wann, C. Stinespring,
D.B. Dadyburjor and J.W. Zondlo
Department of Chemical Engineering
West Virginia University

OBJECTIVES

The major thrusts of the work during 1992-1993 were the construction and testing of the aerosol reactor and the development of the aerosol technique for making mixtures of pyrite (PY) and pyrrhotite (PH) using ferric sulfide precursor. Involved in the development work were the determination of the size and chemistry of the particles produced by the aerosol reactor, the determination of the factors which control particle size and chemistry, and the evaluation of some of the materials formed in the reactor for catalytic activity in coal liquefaction experiments. In related work, catalysts formed by hydrothermal disproportionation of ferric sulfide under a wide range of conditions had previously been characterized using surface and wet-chemical techniques. These results were assembled and compared with the activity of these catalysts to come up with an overall model for the processes going on during hydrothermal disproportionation under a wide range of conditions. Another significant thrust during this period was the surface characterization of catalysts prepared by other members of the consortium.

RESULTS

1. Reactor Construction. The reactor system for the production of microfine iron catalysts has been constructed. The system consists of four basic components: a pump, a fuel injector, the reactor body, and a scrubber. The relation between these four is shown in Figure 1.

The pump is driven by high-pressure air and is capable of pumping up to 1 ml of liquid per cycle at 8800 psi pressure. The cycle rate can be adjusted from 0.011 to 3.3 Hz. The fuel

injector has a pin pressure of 6000 psi. Details of the modifications of this component are given below. The reactor body is essentially a cylinder 1 m long and 250 mm in diameter. The reactor temperature can be raised to 250°C through external band heaters. A sealable flange joins the injector component to the reactor body and enables pressures of up to 300 psig to be maintained in the reactor. The scrubber removes all traces of objectionable species from the exit stream of the reactor before the stream is vented through the hood.

2. Test Runs. The results of our previous work have shown that ferric sulfide disproportionates to PH, PY and elemental sulfur at different ratios, depending upon the time, temperature and pressure of the disproportionation. Those experiments have been in hydrothermal-bomb reactors. One particular mixture, with a PH/PY ratio of 1, has been shown [1,2] to be an effective catalyst for coal liquefaction. This catalyst mixture has been obtained at disproportionation conditions of 200°C and 250 psia, well within the range of the aerosol reactor. Hence these conditions were used for the test runs.

Reactants used to make ferric sulfide for the hydrothermal-bomb reactor were ferric chloride and sodium sulfide. These could not be used in the aerosol reactor. Instead, ferric acetate and hydrogen sulfide were used as reactants in the aerosol reactor. (Using ferric acetate in the hydrothermal-bomb reactor does not result in a catalyst which is significantly different from one made with ferric chloride in the same reactor.) Ferric acetate was prepared by first making ferric hydroxide from ferric chloride and ammonium hydroxide. The precipitate was washed and rinsed with distilled-deionized water to remove the chloride salt and excess ammonium hydroxide. The ferric hydroxide precipitate was then stirred and heated with acetic acid. The experiments were carried out by pumping this solution through the injector into the aerosol reactor.

Before starting the pumping, the reactor was charged with 10 parts of nitrogen to one part of hydrogen sulfide at a pressure of 200 psig and heated to 200°C by the band heaters. During injection, the ferric acetate solution is converted to an aerosol with a droplet diameter of about 50 μ, as estimated from fuel-oil calculations. Ferric ions at the surface of the droplet react almost instantaneously with the hydrogen sulfide in the vapor phase, forming a crust of ferric sulfide on the surface of the droplet. Under the experimental conditions, the ferric sulfide is unstable, and disproportionates into PH and PY. Depending upon the system

pressure, water can be vaporized from the droplet, shrinking the diameter. Under the present conditions, the pressure is near the vapor pressure of water, so the evaporation of water is slowed. Thus the droplet configuration is maintained until all the ferric acetate in the droplet is reacted. The product is essentially a hollow sphere with a crust of PH and PY. This product settles to the bottom of the reactor, where it can be easily flushed out with water after the batch reaction is complete. The other products, acetic acid and steam, are vented from the reactor through a pressure-controlled check valve, and pass through the scrubber. Make-up gas for the reactor in the proper ratio is fed via mass-flow valves at the nitrogen and hydrogen sulfide sources.

In the early test runs, scanning electron microscopy (SEM) analysis of the products showed that many particles of relatively large size (greater than 20 μ) were present. These would correspond to aerosol droplet sizes much larger than 50 μ. Further, excess fluid was seen to be emitted from the leakoff port in the fuel injector, indicative of orifice plugging. In addition, the injector metals were heavily plated with iron sulfides during the reaction, and some pitting of injector parts was also noted. Between injections, the ferric acetate solution evaporated, and crystals of ferric sulfide that were formed prevented the tight re-seating of the injector pin. Hence, in addition to the 50-μ droplets formed by the injector, large drops of solution escaped through the partially-opened orifice.

To avoid this problem, a new nozzle, constructed from 303 Stainless Steel (SS), was purchased. This is a hydraulic hollow-cone atomizer, not a fuel injector, so it has to be backed up by a pressure-check valve. The 303 SS is not reacted by the gases in the reactor during the batch run, and the system seems to be very effective in producing small particles.

3. Product Properties. Samples from the aerosol reactor with the new nozzle were collected and analyzed. SEM analysis shows that the particles are indeed spherical, as expected. They are also hollow. Some shells can be seen resulting from breakage of the hollow spheres. The diameter of the largest spheres is approximately 2 μ, but the surface of the spheres is composed of very fine crystals of size less than 0.1 μ. In addition, SEM indicates a significant quantity of spheres of overall diameter much smaller than 2 μ, which would result in a mean particle diameter of less than 1 μ. Some spheres have surfaces which appear to contain fissures, consistent with the escape of vapor during the shrinking process; other spheres seem

intact.

A second analysis of particle size was carried out using light scattering. A printout of the particle size distribution is reported in Table I. A normal distribution curve is obtained, with a mean diameter of 0.8 μ. This is consistent with the SEM analysis.

A helium pycnometer was used to determine the density of the spherical particles. Samples from several runs were separately examined. The density of every sample was significantly less than that of any known iron sulfide. The average value obtained was 3.78 g/ml, while typical bulk iron sulfides range in density from 4.5 to 5 g/ml. Further, the density of the particles was found to increase when samples were ground. These observations confirm that the particles are indeed hollow spheres.

The particles were chemically analyzed, using the selective acid dissolution technique used earlier by us to differentiate between PH and PY. The analysis shows that the iron sulfide mixtures produced by the aerosol reactor are indeed 50-50 mixtures of PY and PH, in agreement with the ratio corresponding to the sample produced in the hydrothermal-bomb reactor under the same conditions.

X-ray diffraction (XRD) studies of the aerosol products were carried out in the laboratory of Professor M.S. Seehra. The results (Figure 2) show clearly a diffraction pattern for PY but not for PH. This is also consistent with XRD analysis of the hydrothermally produced product. In fact, the XRD patterns are nearly identical. As in the hydrothermally produced material, the PH is small enough to be transparent or amorphous to X rays.

Surface area measurements of the aerosol products by BET indicate a value of 9.52 m^2/g. This is consistent with the average particle size reported above.

4. Controlling Factors. The temperature of the aerosol reactor is expected to control the rate of formation of ferric sulfide, but this is believed to be so rapid that temperature should have relatively little effect in this regard. However, the temperature should control the relative distribution of PH and PY, following the results for the hydrothermally produced material (summarized below). The effect of temperature has not yet been extensively studied in the aerosol reactor.

A preliminary study of the effect of reactor pressure has been carried out for the aerosol material. Particles produced at a lower pressure (100 psig as compared to 200 psig) have a

higher density, 4.6 g/ml as compared to 3.78 g/ml. The higher density falls in the range of bulk densities expected, implying that these particles are more solid (less hollow) than those obtained at the higher pressure. A lower reactor pressure can be expected to increase the rate of vaporization of water; if this rate is of the order of the rate of formation of the ferric sulfide, then more-solid particles can be expected to be obtained.

The effect of the concentration of the ferric acetate has also been preliminarily investigated. For a 0.1M solution, the maximum particle size was found to be 11.5 μ, whereas a similar measurement starting with a 0.01M solution yields 5 μ. A more- dilute solution of precursor corresponds to smaller amounts of ferric acetate (and ferric sulfide) per droplet, lower rates of reaction, and smaller particles.

5. Activity and Yield for Coal Liquefaction. Experiments have been run to test the activity and yield of the particles produced by the aerosol reactor. Liquefaction reactions were carried out at 350°C and 1000 psig hydrogen pressure for 1 h at a shaking speed of 500 rpm. The total conversion was found to be 70%, with a yield of 6.4% oil (+ gas). These numbers are comparable to those with the hydrothermally disproportionated catalyst

6. Hydrothermally Disproportionated Catalyst. Results from XRD, Auger electron spectroscopy (AES), and wet chemical analysis before and after liquefaction, have been combined with the phase diagram of the Fe-S system and the liquefaction results to obtain an overall picture of the hydrothermally disproportionated catalysts obtained under a wide range of preparation conditions. The full results have been summarized elsewhere [3]. However, the following comments can be made.

From the phase diagram [4], Fe_2S_3 is unstable, at least above 0°C. At 25°C, a solid mixture of PY (FeS_2) and greigite (Fe_3S_4) is expected to be thermodynamically stable. At 100°C and 200°C, solid mixtures of PY and monoclinic pyrrhotite (Fe_7S_8) are expected thermodynamically, while mixtures of PY and troilite (FeS) are expected above 250°C.

For the disproportionation of Fe_2S_3 for 1 h at room temperature, therefore, we expect the main reaction to be

$$Fe_2S_3 \rightarrow 0.67\ Fe_3S_4 + 0.33\ S$$

After liquefaction at 350°C, the following change takes place in the disproportionated catalyst:

$$Fe_3S_4 \rightarrow 2\ FeS + FeS_2$$

If the liquefaction is carried out at 400°C, the above reaction is followed by the increasingly important reaction:

$$FeS_2 + 2H_2 \rightarrow FeS + 2\ H_2S$$

For disproportionation at 100°C, the data are consistent with:

$$Fe_2S_3 \rightarrow 0.18\ Fe_7S_8 + 0.73\ FeS_2 + 0.09\ S$$

After liquefaction at 350°C using this catalyst,

$$FeS_2 + H_2 \rightarrow FeS + 2\ H_2S$$

whereas for liquefaction at 400°C,

$$Fe_7S_8 \rightarrow FeS_2 + 6\ FeS$$

Finally, disproportionation at 200°C requires elemental S to be a (net) reactant, following

$$Fe_2S_3 + 0.2\ S \rightarrow 0.13\ Fe_7S_8 + 1.1\ FeS_2$$

After liquefaction at 350°C or 400°C,

$$Fe_7S_8 \rightarrow FeS_2 + 6\ FeS$$

As mentioned earlier, all these processes are consistent with data from wet chemical analyses before and after liquefaction, XRD and AES.

The effects of catalyst loading on the overall conversion and product yield for coal liquefaction were also investigated. These reactions were carried out using DECS-17 coal and the 200°C-disproportionated catalyst, presulfided with 0.1 ml CS_2. The reaction temperature was 350°C and 1000 psig (cold) of hydrogen was used in the batch reactor. For a batch time of 1 h, the results are summarized in Figure 3. Conversion and oil (+ gas) yield are seen to vary nonlinearly with catalyst loading. The conversion increases with loading up to approximately 0.6 percent Fe; at higher loadings, the conversion continues to increase, but to a lesser extent. At low catalyst loadings, the yield of oil (+ gas) is less than under non-

catalytic conditions. The yield is a minimum around 0.6 percent Fe loading, after which the yield increases. Clearly the catalyst not only converts coal to preasphaltenes and asphaltenes, but is also instrumental in converting oils into heavier products by retrograde reactions.

Such reactions are expected to be minimized in a flow-through reactor, where the contact time is of the order of seconds rather than 1h, as in the batch case. One such flow-through reactor is currently undergoing testing, as reported in Task I.6. Under such conditions, the optimum catalyst loading is expected to be around 1 percent, corresponding to the leveling-off of the steep conversion-loading curve of Figure 3.

7. Measurement of Gas Yields from Batch Reactors. In analyzing the products from liquefaction reactions to date, we have found that the minimum error is obtained when the amounts of unconverted coal and asphaltenes/preasphaltenes are measured directly, and the amounts of oil (+ gas) are obtained by difference. (Details of the procedure are given in, e.g., ref. [2].) However, this means that the amounts of oil and gas cannot be separately obtained. Visual examination has led us to believe that the amount of gas products is small, so that the yield can be taken as that of the oil alone, but to date this has not been verifiable. This year, we have developed a technique to quantify the amount of gas products formed after liquefaction, and have used this technique in a representative number of runs.

After the reactor is cooled to room temperature following the run, a specially-designed attachment is connected to the stem of the reactor, and the vapor flows through a collector maintained at liquid nitrogen temperatures. This condenses almost all of the vapor, except hydrogen. When all the vapor from the reactor has been passed through, the collector is sealed and heated, and the contents are flushed through a gas chromatograph with a thermal conductivity detector. Calibration of the detector signal allows us to quantify the nature and amount of each component in the vapor.

The results indicate that the vapor contains mainly C_2 species. Table II shows some quantitative results from liquefaction experiments. In all cases, the amount of gas is less than 15 percent of the total oil + gas yield, confirming our earlier expectation. The total amount of gas produced increases with increasing liquefaction temperature. The relative amounts of gas and oil are roughly constant with temperature. Further, both the total amount of gas and the amount relative to oil decrease with increasing reaction time. This latter observation is

consistent with the earlier comment regarding retrograde condensation of oil and gas to asphaltenes and preasphaltenes. The gas would appear to be preferentially condensed.

8. Surface Characterization of Other Consortium Catalysts. Research activities here focused on Auger electron spectroscopy (AES) analyses of sulfated iron oxide (SIO) catalyst particles. The samples were supplied by the University of Pittsburgh and were previously used by us in comparative studies of liquefaction. The samples were identified as Fe_2O_3/SO_4^{2-} and Fe_2O_3/SO_4^{2-} with 1% Mo.

No optical or SEM analyses were performed. However, it was evident that the SIO particles, like the hydrothermally disproportionated catalyst, were extremely small. Also like the hydrothermally disproportionated catalyst, the SIO catalyst was only lightly contaminated by carbon, as could be seen by AES. For both samples of the SIO catalyst, the O/Fe ratio ranges from a nominal 1.5 to 1.9. The S/Fe ratio was found to be 0.1 to 0.2. These contrast sharply with the hydrothermally disproportionated catalyst, where O/Fe was found to be 1 and S/Fe was found to be 2, with essentially half the S being associated with excess elemental sulfur left over from the disproportionation process.

Line-shape analyses showed that the Fe-MVV AES peak is consistent with that of the Fe_2O_3 standard. Because of the low intensity of the S-LVV peak, a meaningful analysis of the line shape of this portion was difficult to obtain.

Other activities in this thrust consisted of refurbishing the existing AES system, and developing new facilities for x-ray photoelectron spectroscopy (XPS). These activities are significant to the program for several reasons. Repairs to the existing AES system allow the electron gun to be operated at substantially lower beam currents, while maintaining an acceptable signal-to-noise level. This minimizes the damage induced by the electron beam, which can alter the surface composition and stoichiometry. Further, the XPS facility being developed will provide more clear-cut information on the chemical states of metal and sulfur species in the catalyst particles. This capability is essential as we move to catalysts with more complex compositions, as discussed below.

FUTURE WORK

The effect of solution concentration, injection pressure, reactor pressure and temperature

on the properties of the aerosol catalysts, particularly their size and density, will be investigated. Mixed metal catalysts will be produced by this technique. The physical and catalytic properties of these materials will be investigated. The surface characterization of aerosol catalysts, both those containing iron alone and those containing mixed metals, will be investigated. Co-liquefaction of coal with waste materials will be investigated.

REFERENCES

1. Stansberry, P.G., J. Yang and J.-P. Wann, AIChE Ann. Mtg. (1991).

2. Stansberry, P.G., J.-P. Wann, W.R. Stewart, J. Yang, J.W. Zondlo, A.H. Stiller and D.B. Dadyburjor, Fuel 72, 793 (1993).

3. Dadyburjor, D.B., W.R. Stewart, A.H. Stiller, C.D. Stinespring, J.-P. Wann and J.W. Zondlo, Energy & Fuels, submitted (1993).

4. Power, L.F. and H.A. Fine, Miner. Sci. Eng. 8, 106 (1976).

TABLE I

Particle Size Distribution of Aerosol Disproportionated Catalyst

Under, %	Size, μ
25	0.58
50	0.79
65	0.99
70	1.11
75	1.26
80	1.47
85	1.77
90	2.37
95	3.37
99	5.00

TABLE II

Liquefaction Results Including Separate Gas Yields
(DECS-6 Coal, 0.1 ml CS_2, 1000 psig H_2, 500 rpm)

Temp °C	Time h	Conversion %	Asphaltene %	Oil %	Gas %
350	0.5	55.7	43.8	10.3	1.6
	1.0	57.2	46.6	9.9	0.76
400	0.5	88.2	60.2	24.8	3.2
	1.0	92.8	60.1	30.0	2.7

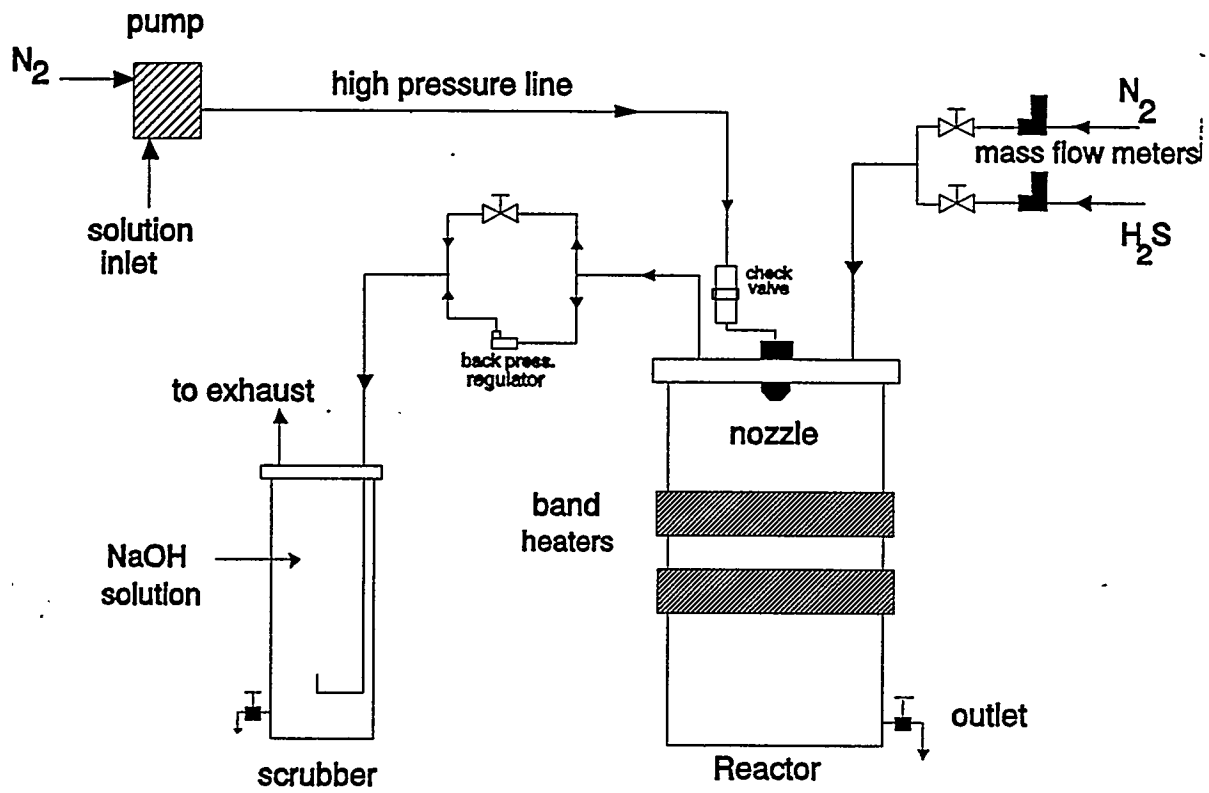

Figure 1. Schematic of system for aerosol catalyst manufacture.

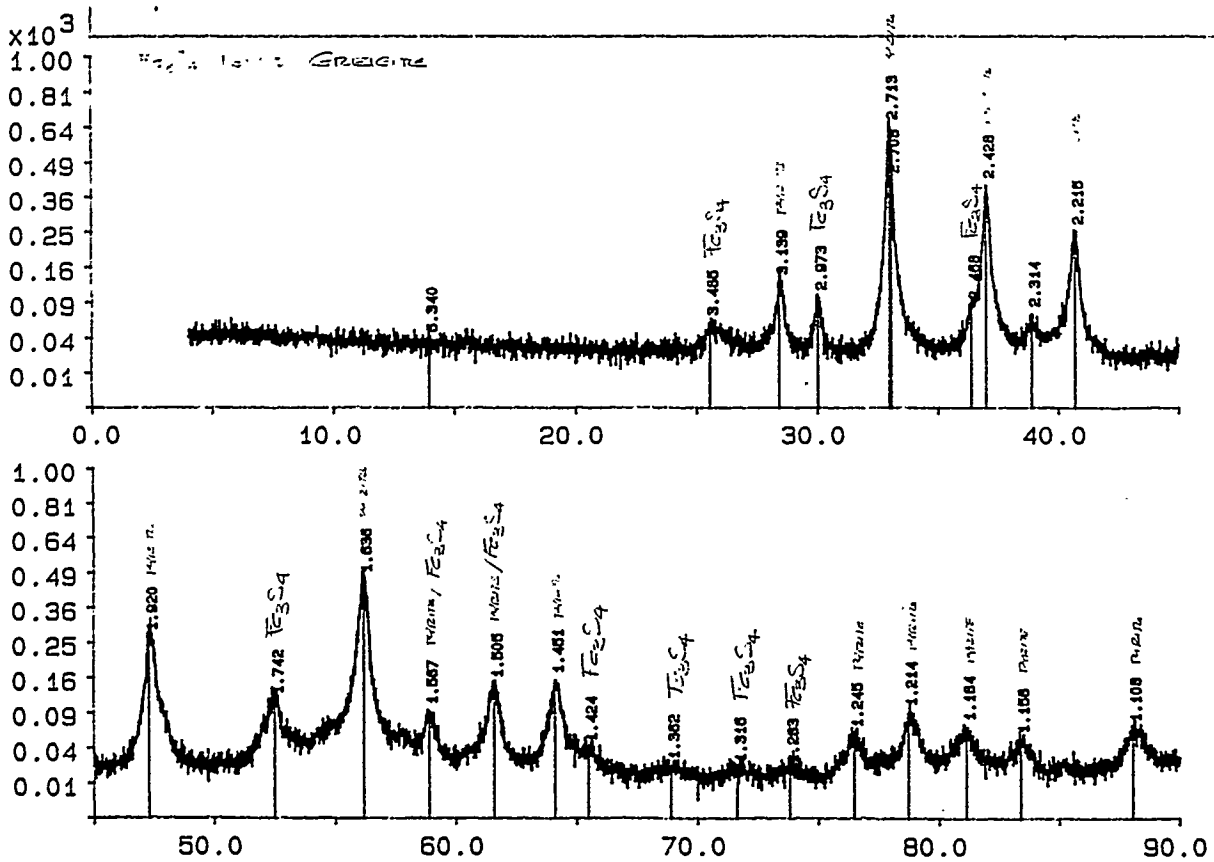

Figure 2. X-ray diffraction pattern for aerosol catalyst.

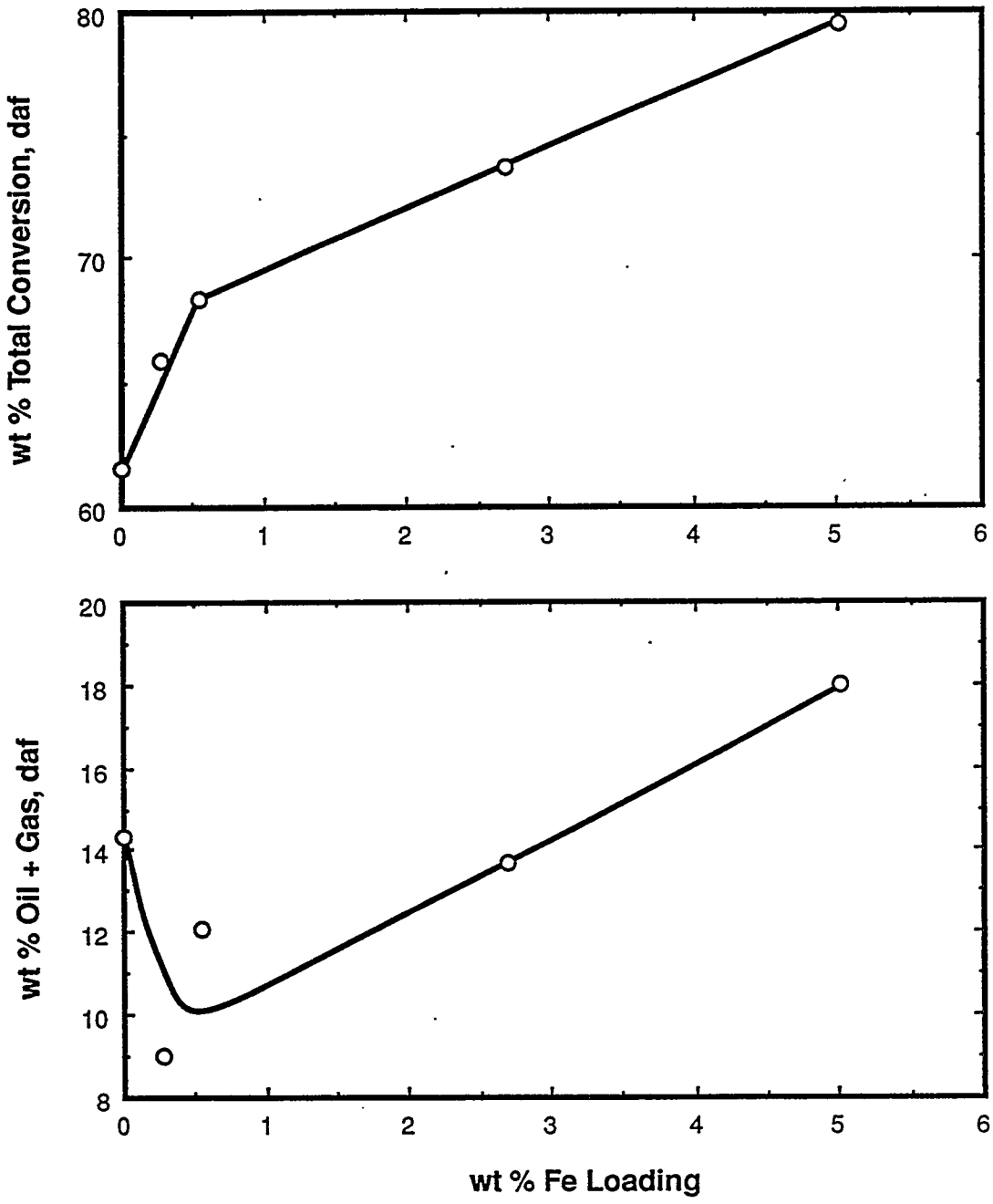

Figure 3. Effect of loading (of 200°C-hydrothermally disproportionated catalyst) on conversion and oil (+ gas) yield